in *Conf. Rec. International Conference on the Applications of Photonic Technology 4 (ICAPT 2000)*, vol. 4087, (Roger A. Lessard and George A. Lampropoulos, eds.), pp. 379-388, Québec City, QC, Canada: SPIE, June 12-16, 2000.

Pulse Narrowing in Optical Components with Polarization Mode Dispersion Using Polarization Controls

Liang Chen[a] , Mauricio Yañez[b], Xiaoyi Bao[a] and Brent R. Petersen[b]

[a] Physics Department, University of New Brunswick, Fredericton, NB E3B 5A3
[b]Department of Electrical and Comp. Engineering, University of New Brunswick

ABSTRACT

An algorithm capable of finding the input and output states of polarization for maximum pulse narrowing at the output of an optical fiber with polarization mode dispersion (PMD) is analytically presented and numerically solved. It is always possible to obtain output pulses which are narrower than the input pulses when PMD is compensated by controlling both the input polarization as well as the receiver polarization states. This anomalous effect was shown to be exclusively due to PMD as no chromatic dispersion or polarization dependent losses were assumed. We report the detailed study for the cases in which the fiber consists of two, three and five hundred segments of highly-birefringent (Hi-Bi) fiber. The solution shows the existence of two orthogonal input and output states of polarization (different from those introduced by Poole et. al.) under which the integrity of the pulse is preserved and the pulsewidth at the output is the narrowest possible. The cost to be paid for this improvement is a reduction of the optical power in the output pulse.

Keywords: Polarization Mode Dispersion, Pulse Narrowing, States of Polarization

1. INTRODUCTION

Polarization mode dispersion (PMD) may introduce unacceptable levels of signal degradation in high speed (10 Gbps) optical communication systems. The signal degradation takes the form of pulse broadening due to the differential transmission time of two pulses polarized along orthogonal states of polarization (SOP). This kind of PMD is commonly known as first order PMD[1]. A series of PMD compensation methods[2-6] have been proposed in order to overcome the problem. Under first order PMD, a pulse at the input of a fiber can be decomposed into two pulses with orthogonal SOP. Both pulses will arrive at the output of the fiber undistorted and polarized along different SOP, the output SOP being orthogonal. The differential transmission time between those pulses is referred to as Differential Group Delay, DGD, and the input (output) SOP which allow the transmission (reception) of undistorted pulses are known as the Principal input (output) States of Polarization (PSPs)[1]. Both, the PSPs and the DGD are assumed to be frequency independent when only first order PMD is being considered.

Second order PMD effects account for the frequency dependence of the DGD and the PSPs. The frequency dependence of the DGD introduces an effective chromatic dispersion of opposite sign on the signals polarized along the output PSPs. It is possible to obtain output pulses which are narrower than the input pulses when the DGD depends on frequency and when the transmitted pulse is chirped[7]. Until recently,[8] this was the only way of obtaining a beneficial pulse narrowing effect in optical fibers suffering from PMD.

One simple method of doing first order PMD compensation consists of either transmitting the signal on one of the input PSPs[9] or receiving the signal on one of the output PSPs[2,8,9]. The underlying idea being the introduction of a change in the frequency response of the fiber in a way such that only one pulse propagates through the fiber (PSP transmission) or is detected at the receiver (PSP reception). The dependence of the frequency response of the fiber on the input and output SOP has led to the conclusion that it is possible to obtain output pulses which are narrower than the input pulses (without the introduction of a chirp in the transmitted pulse) by properly adjusting the input and output SOP[8].

Here, we leverage the use of that dependence in order to minimize the rms-pulsewidth of a signal at the fiber output. In section two, we outline the mathematical analysis required in that direction. In section three an algorithm capable of searching

for the input and output SOP in which the smallest rms-pulsewidth can be generated is described. In section four, through computer simulation we present the existence of two mutually orthogonal input and output SOP, under which the absolute minimum rms-pulsewidth can be obtained. Section five gives a brief summary and conclusions.

2. PULSEWIDTH ANALYSIS

A time varying electric field at the input of an optical fiber can be represented[10] in the frequency domain as

$$\mathbf{E_{in}} = E_{in}(\omega)\mathbf{j} \tag{1}$$

where ω is the optical frequency and we have neglected the initial phase; $\mathbf{j}$ is a 2 by 1 Jones vector representing the input state of polarization. $E_{in}(\omega)$ is the Fourier transform of $E_{in}(t)$ given by

$$E_{in}(\omega) = \frac{1}{\sqrt{2\pi}} \int_{-\infty}^{\infty} E_{in}(t) e^{-j\omega t} dt \quad . \tag{2}$$

If we treat an optical fiber with PMD as a linear medium without polarization dependent losses, we can represent it by a 2 by 2 complex matrix given by[1]

$$\mathbf{T}(\omega) = e^{j\beta(\omega)}\mathbf{U}(\omega) \tag{3}$$

where $\beta(\omega)$ accounts for the chromatic dispersion and $U(\omega)$ is a unitary matrix. The complex lowpass[16] transfer matrix can simply be obtained as

$$\mathbf{T_L}(\omega) = \mathbf{T}(\omega + \omega_o) = e^{j\beta(\omega+\omega_o)}\mathbf{U}(\omega + \omega_o) \tag{4}$$

where ω_o is the optical carrier frequency. Thus, the signal at the fiber output is obtained by multiplying equations 1 and 4,

$$\mathbf{E_{out}} = \mathbf{T_L}(\omega) E_{in}(\omega)\mathbf{j} \quad . \tag{5}$$

In general, different frequency components of $\mathbf{E_{out}}$ will have different polarization states at the output of the fiber. By using a Polarization Analyzer (PA) it is possible to project all the frequency components of $\mathbf{E_{out}}$ onto a particular state of polarization. This is referred to as *receiving the signal on a particular state of polarization.* Therefore, the result of receiving $\mathbf{E_{out}}$ on a state of polarization $\mathbf{c}$ will be

$$E_\chi(\omega) = \mathbf{c}^{+}\mathbf{E_{out}} = \mathbf{c}^{+}\mathbf{T_L}(\omega)\mathbf{j}\,E_{in}(\omega) \tag{6}$$

where the output state of polarization, $\mathbf{c}$ is another 2 by 1 Jones vector and "+" represents the transpose complex conjugate (Hermitian) of a matrix or a vector.

We define the rms-pulsewidth[10] of $E_\chi(\omega)$, σ_χ as

$$\sigma_\chi^2 = \langle t^2 \rangle - \langle t \rangle^2 \tag{7}$$

where the n-th moment of t in the time domain is given by[11]

$$\langle t^n \rangle = \frac{\int_{-\infty}^{\infty} E_\chi^*(t) t^n E_\chi(t) dt}{\int_{-\infty}^{\infty} \left| E_\chi(t) \right|^2 dt} \tag{8}$$

where $E_\chi(t)$ is the inverse Fourier transform of $E_\chi(\omega)$ defined as

$$E_\chi(t) = \frac{1}{\sqrt{2\pi}} \int_{-\infty}^{\infty} E_\chi(\omega) e^{j\omega t} d\omega \tag{9}$$

and the superscript * denotes complex conjugate.

By using Fourier transform and Parseval's theorem it is easy to prove that the first two moments of t can be expressed in the frequency[10] domain as

$$< t > \; = \; \frac{j \int_{-\infty}^{\infty} E_\chi^*(\omega) \frac{dE_\chi(\omega)}{d\omega} d\omega}{\int_{-\infty}^{\infty} \left| E_\chi(\omega) \right|^2 d\omega} \tag{10.1}$$

and

$$< t^2 > \; = \; \frac{\int_{-\infty}^{\infty} \left| \frac{dE_\chi(\omega)}{d\omega} \right|^2 d\omega}{\int_{-\infty}^{\infty} \left| E_\chi(\omega) \right|^2 d\omega} \quad . \tag{10.2}$$

Substituting eqs. 6 and 10 into eq. 7 we obtain a final expression for σ_χ^2 as a function of $\mathbf{j}$ and $\mathbf{c}$,

$$\sigma_\chi^2(\mathbf{j},\mathbf{c}) = \frac{\int_{-\infty}^{\infty} \mathbf{c}^+ \left[\frac{d}{d\omega} \mathbf{T_L}(\omega) E_{in}(\omega) \right] \mathbf{j}\,\mathbf{j}^+ \left[\frac{d}{d\omega} \mathbf{T_L}^+(\omega) E_{in}^*(\omega) \right] \mathbf{c}\, d\omega}{\int_{-\infty}^{\infty} \mathbf{c}^+ \mathbf{T_L}(\omega)\, \mathbf{j}\,\mathbf{j}^+ \mathbf{T_L}^+(\omega)\, \mathbf{c} \left| E_{in}(\omega) \right|^2 d\omega}$$

$$- \left\{ \frac{j \int_{-\infty}^{\infty} \mathbf{c}^+ \left[\frac{d}{d\omega} \mathbf{T_L}(\omega) E_{in}(\omega) \right] \mathbf{j}\,\mathbf{j}^+ \mathbf{T_L}^+(\omega) E_{in}^*(\omega) \mathbf{c}\, d\omega}{\int_{-\infty}^{\infty} \mathbf{c}^+ \mathbf{T_L}(\omega)\, \mathbf{j}\,\mathbf{j}^+ \mathbf{T_L}^+(\omega) \left| E_{in}(\omega) \right|^2 \mathbf{c}\, d\omega} \right\}^2 . \tag{11}$$

Instead of trying to find the values of $\mathbf{j}$ and $\mathbf{c}$ which minimize eq. 11, we will break up the minimization problem into two separate minimization sub-problems. This is done for the sake of simplifying the calculations. First, we assume that the input state of polarization, $\mathbf{j}$, is fixed and search for the optimum output state of polarization, $\mathbf{c_{opt}}$, which minimizes the rms-pulsewidth for a given output state of polarization, $\sigma_\chi^2(\mathbf{c})$. Then, the problem is reversed and we search for the optimum input state of polarization, $\mathbf{j_{opt}}$, which minimizes the rms-pulsewidth for a given input state of polarization, $\sigma_\chi^2(\mathbf{j})$, while assuming $\mathbf{c}$ is fixed. In both cases, the constraint imposed on the minimization process is that the 2 by 1 complex vector representing the input or output state of polarization corresponds to a Jones vector, i.e., $\mathbf{j}^+\mathbf{j} = 1$ and $\mathbf{c}^+\mathbf{c} = 1$ respectively.

After simplifying the notation and by using Lagrange multipliers to enforce the minimization constraint, we get[12]

$$\left[\frac{\mathbf{S}_\varphi}{\overline{P}} - \frac{\mathbf{P}_\varphi \mathbf{c}\mathbf{c}^+ \mathbf{S}_\varphi}{\overline{P}^2} - 2\frac{\mathbf{T}_\varphi \mathbf{c}\mathbf{c}^+ \mathbf{T}_\varphi}{\overline{P}^2} + 2\overline{T}\frac{\mathbf{P}_\varphi \mathbf{c}\mathbf{c}^+ \mathbf{T}_\varphi}{\overline{P}^3} \right] \mathbf{c} = \eta\, \mathbf{c} \tag{12.1}$$

$$\left[\frac{\mathbf{S}_\chi}{\overline{P}} - \frac{\mathbf{P}_\chi \mathbf{j}\mathbf{j}^+ \mathbf{S}_\chi}{\overline{P}^2} - 2\frac{\mathbf{T}_\chi \mathbf{j}\mathbf{j}^+ \mathbf{T}_\chi}{\overline{P}^2} + 2\overline{T}\frac{\mathbf{P}_\chi \mathbf{j}\mathbf{j}^+ \mathbf{T}_\chi}{\overline{P}^3} \right] \mathbf{j} = \lambda\, \mathbf{j} \quad . \tag{12.2}$$

The terms within brackets in eq. 12 represent a 2 by 2 complex matrix. Equation 12.1 represents the case in which $\mathbf{j}$ is fixed and $\mathbf{c}$ is varied, whilst eq. 12.2 represents the opposite case. In eq. 12, η and λ are the Lagrange multipliers. The newly introduced terms are defined as[12]

$$\left.\begin{aligned}
\mathbf{P}_\varphi &= \int_{-\infty}^{\infty} \mathbf{T}_L(\omega)\,\mathbf{j}\,\mathbf{j}^{+}\mathbf{T}_L^{+}(\omega)\left|E_{in}(\omega)\right|^2 d\omega \\
\mathbf{P}_\chi &= \int_{-\infty}^{\infty} \mathbf{T}_L^{+}(\omega)\,\mathbf{c}\,\mathbf{c}^{+}\mathbf{T}_L(\omega)\left|E_{in}(\omega)\right|^2 d\omega \\
\mathbf{T}_\varphi &= j\int_{-\infty}^{\infty}\left[\frac{d}{d\omega}\mathbf{T}_L(\omega)E_{in}(\omega)\right]\mathbf{j}\,\mathbf{j}^{+}\mathbf{T}_L^{+}(\omega)E_{in}^{*}(\omega)d\omega \\
\mathbf{T}_\chi &= j\int_{-\infty}^{\infty}\mathbf{T}_L^{+}(\omega)E_{in}^{*}(\omega)\,\mathbf{c}\,\mathbf{c}^{+}\left[\frac{d}{d\omega}\mathbf{T}_L(\omega)E_{in}(\omega)\right]d\omega \\
\mathbf{S}_\varphi &= \int_{-\infty}^{\infty}\left[\frac{d}{d\omega}\mathbf{T}_L(\omega)E_{in}(\omega)\right]\mathbf{j}\,\mathbf{j}^{+}\left[\frac{d}{d\omega}\mathbf{T}_L^{+}(\omega)E_{in}^{*}(\omega)\right]d\omega \\
\mathbf{S}_\chi &= \int_{-\infty}^{\infty}\left[\frac{d}{d\omega}\mathbf{T}_L^{+}(\omega)E_{in}^{*}(\omega)\right]\mathbf{c}\,\mathbf{c}^{+}\left[\frac{d}{d\omega}\mathbf{T}_L(\omega)E_{in}(\omega)\right]d\omega \\
\overline{T} &= \mathbf{c}^{+}\mathbf{T}_\varphi\,\mathbf{c} = \mathbf{j}^{+}\mathbf{T}_\chi\,\mathbf{j} \\
\overline{P} &= \mathbf{c}^{+}\mathbf{P}_\varphi\,\mathbf{c} = \mathbf{j}^{+}\mathbf{P}_\chi\,\mathbf{j}
\end{aligned}\right\}. \qquad (13)$$

3. SEARCHING ALGORITHM

In order to find the optimum values of $\mathbf{j}$ and $\mathbf{c}$ we need to solve eq. 12.1 and 12.2 jointly. Equation 12 consists of a set of eigenvalue equations and can be rewritten as

$$\left[\mathbf{M}_1(\mathbf{j},\mathbf{c})\right]\mathbf{c} = \eta\,\mathbf{c} \qquad (14.1)$$

$$\left[\mathbf{M}_2(\mathbf{j},\mathbf{c})\right]\mathbf{j} = \lambda\,\mathbf{j} \qquad (14.2)$$

where $\mathbf{M_1}$ and $\mathbf{M_2}$ are complex 2 by 2 matrices which correspond to the terms within the brackets in equations 12.1 and 12.2 respectively. At the beginning of the search, an arbitrary set of input and output SOP, $\mathbf{j_o}$ and $\mathbf{c_o}$, is chosen. The initial set of SOP is used to solve[†] eq. 14.1. The solution of equation 14.1gives two new output SOP, $\mathbf{c_1}$ and $\mathbf{c_2}$. The objective function that we are trying to minimize, σ_χ^2, is then calculated for the two new output SOP along with $\mathbf{j_o}$, $\sigma_\chi^2(\mathbf{j_o},\mathbf{c_1})$ and $\sigma_\chi^2(\mathbf{j_o},\mathbf{c_2})$. The output state of polarization rendering the smallest value of σ_χ^2 will become the new initial output state of polarization, $\mathbf{c_o}$. Next, eq. 14.2 is solved by using $\mathbf{j_o}$ and $\mathbf{c_o}$. Two new input SOP, $\mathbf{j_1}$ and $\mathbf{j_2}$ will be obtained. The objective function is calculated for $\sigma_\chi^2(\mathbf{j_1},\mathbf{c_o})$ and $\sigma_\chi^2(\mathbf{j_2},\mathbf{c_o})$. The input state of polarization yielding the smallest value of σ_χ^2, becomes the new initial value of $\mathbf{j_o}$. At this point one full iteration has finished and the process is repeated, i.e., we repeatedly solve eq. 14.1 followed by eq. 14.2.

[†]The choice of solving eq. 14.1 first as opposed to eq. 14.2 is somewhat arbitrary. The final result for $\mathbf{j_{opt}}$ and $\mathbf{c_{opt}}$ should not be affected by solving eq. 14.2 first.

The searching process will stop when the input and output SOP obtained in the current iteration are almost the same as those obtained in the previous iteration. The input and output SOP obtained during the last iteration are assumed to be $\mathbf{j}_{opt}$ and $\mathbf{c}_{opt}$ respectively. Thus, the rms-pulsewidth of the output pulse, σ_χ, will be the smallest for a given $\mathbf{T}_L(\omega)$ when the pulse is transmitted on a state of polarization $\mathbf{j}_{opt}$ at the input of the fiber and received on a state of polarization $\mathbf{c}_{opt}$ at the output of the fiber.

4. COMPUTER SIMULATION

In this section we use the searching algorithm introduced in section three to minimize the rms-pulsewidth of a Gaussian pulse transmitted through an optical fiber with PMD. It is noteworthy to mention that the mathematical analysis presented in section two did not make simplifying assumptions about the shape of the input signal or the orders of PMD involved. The input normalized electric field in the frequency domain is given by[12]

$$E_{in}(\omega) = \sqrt{\sigma_{in}}\left(\frac{2}{\pi}\right)^{\frac{1}{4}} e^{-(\sigma_{in}\omega)^2} \tag{15}$$

where we choose, σ_{in} = 25 picoseconds, ps, as the rms-pulsewidth of the input pulse. As we want to focus on the impact of the input and output SOP on the pulsewidth of a signal at the output of an optical fiber with PMD only, we neglect the influence of chromatic dispersion, $\beta(\omega)$, in eq. 4. In all the simulations performed, the optical carrier frequency used was ω_o = 1216.1 rad/ps, which corresponds to a carrier wavelength of 1.55 μm.

We begin by considering a fiber made up of three sections of Hi-Bi fiber with different fusion angles between them and each one introducing a DGD of $\tau_0 = \tau_1 = \tau_2$ = 15ps, as shown in Figure 1.

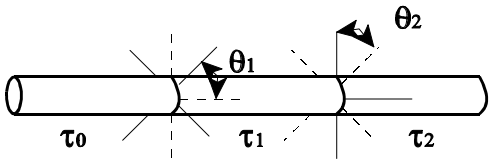

Figure 1 Three Segment System.

where θ_2 is measured with respect to θ_1. The effective pulsewidth is defined as the difference between the output and input rms-pulsewidths,

$$\sigma_{eff} = \sigma_\chi - \sigma_{in} \tag{16}$$

and the power of the output signal polarized along $\mathbf{c}$ is given by

$$P_\chi = \int_{-\infty}^{\infty} \left|E_\chi(\omega)\right|^2 d\omega. \tag{17}$$

Initially the third segment was rotated 45° while the other two remained fixed ($\theta_1 = 0°$ and $\theta_2 = 45°$), the search algorithm was then used to find $\mathbf{j}_{opt}$ and $\mathbf{c}_{opt}$. A minimum value of σ_χ = 19.147 ps was obtained, which accounts for a net reduction of 5.853 ps with respect to σ_{in}. Figure 2 shows the normalized input and output pulses. The narrowing in the pulsewidth of the output signal is achieved at the expense of a sensible decrease in its power.

Figures 3 and 4 show the final values for $\mathbf{j}_{opt}$ and $\mathbf{c}_{opt}$ on the surface of the Poincaré sphere after starting the search from several different input and output SOP.

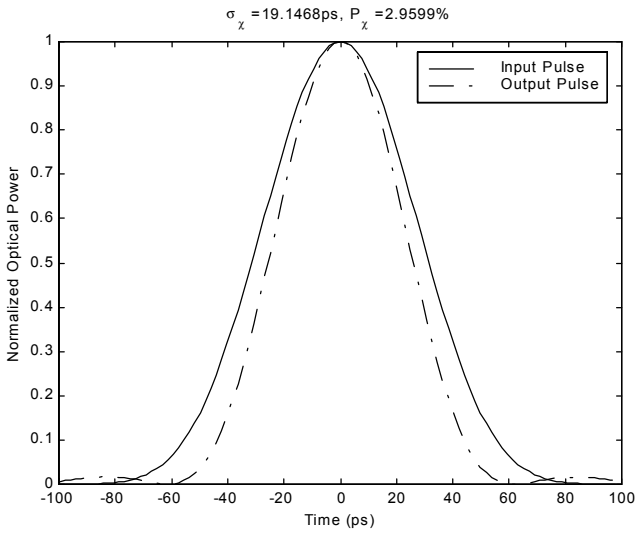

Figure 2 Input pulse and optimized output pulse when $\theta_1 = 0^o$ and $\theta_2 = 45^o$.

In figures 3 and 4 we can appreciate the existence of two different values of $\boldsymbol{\varphi_{opt}}$ and $\boldsymbol{\chi_{opt}}$ respectively. These values lie on diametrically opposite sides of the Poincaré sphere and are therefore orthogonal.

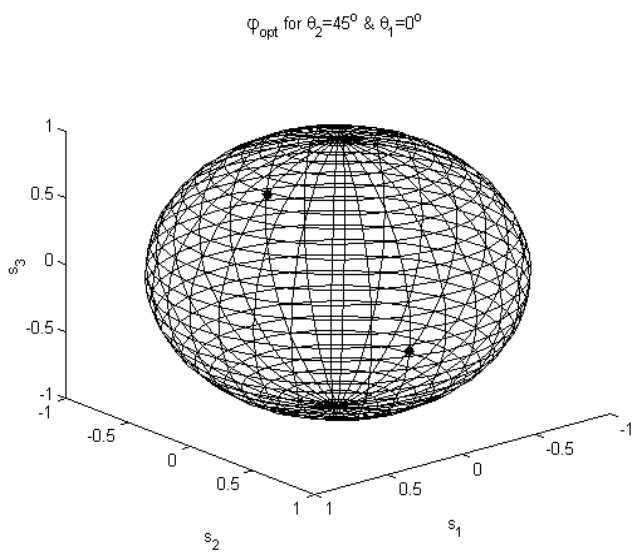

Figure 3 Search results for the input state of polarization showing two independent SOP which produce optimum rms-pulsewidth at the output of the fiber.

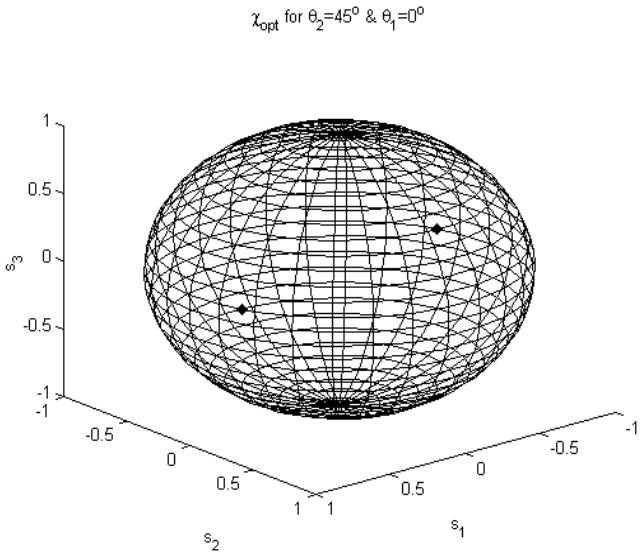

Figure 4 Search results for the output state of polarization showing two independent SOP which produce optimum rms-pulsewidth at the output of the fiber.

To study the influence of the fusion angle θ_2 on the minimum rms-pulsewidth reachable, θ_2 was varied from 10^o to 80^o with 1^o increments and the search algorithm was used to find the minimum σ_χ for each value of θ_2. Figure 5 shows the dependence of σ_{eff} and P_χ on θ_2.

The small scale of the variations of σ_{eff} with changes in θ_2 can be readily explained by looking at the evolution of $\boldsymbol{\varphi_{opt}}$ and $\boldsymbol{\chi_{opt}}$ with the fusion angle. Such evolution is represented on the surface of the Poincaré sphere in figures 6 and 7.

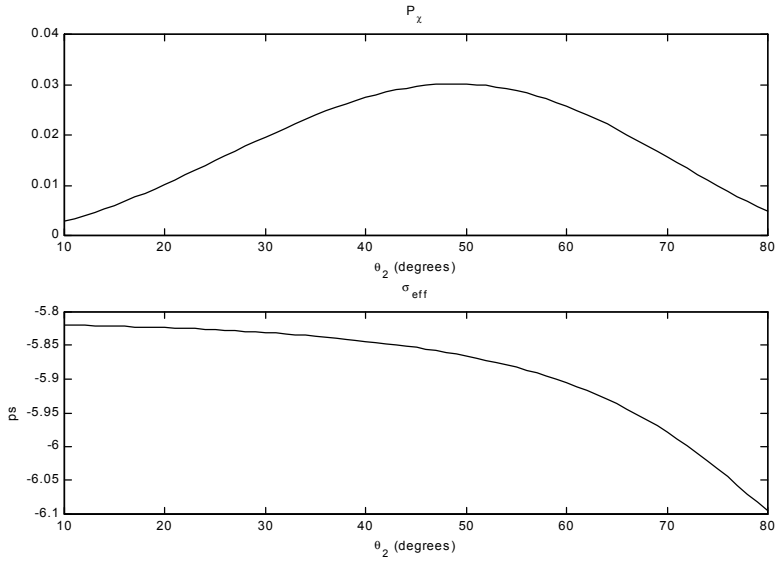

Figure 5 Dependence of σ_{eff} and P_χ on the fusion angle θ_2.

The change introduced in $\mathbf{T}_L(\omega)$ by varying θ_2 tends to be compensated by adequately adjusting φ and χ so that similar value of σ_χ is obtained. Figures 6 and 7 also show the existence of two mutually orthogonal values of φ_{opt} and χ_{opt} for each increment of θ_2. Although there seems to be some influence of the fusion angle on the power of the output signal, P_χ, it remains at a very low level, $\leq 3\%$.

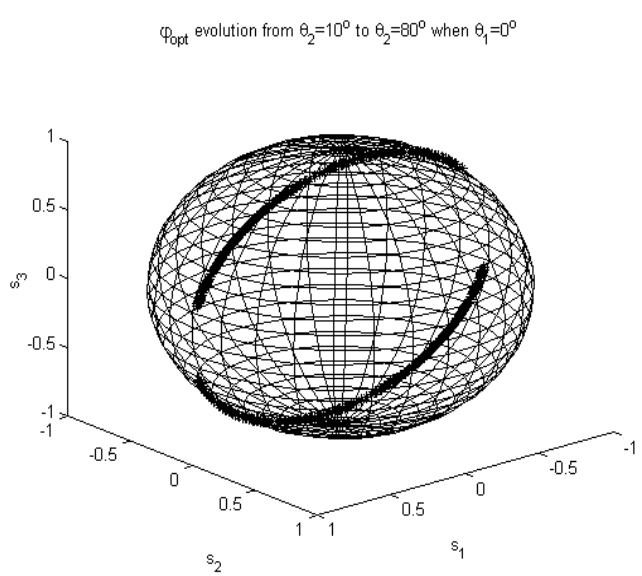

Figure 6 Optimum input state of polarization evolution with the fusion angle.

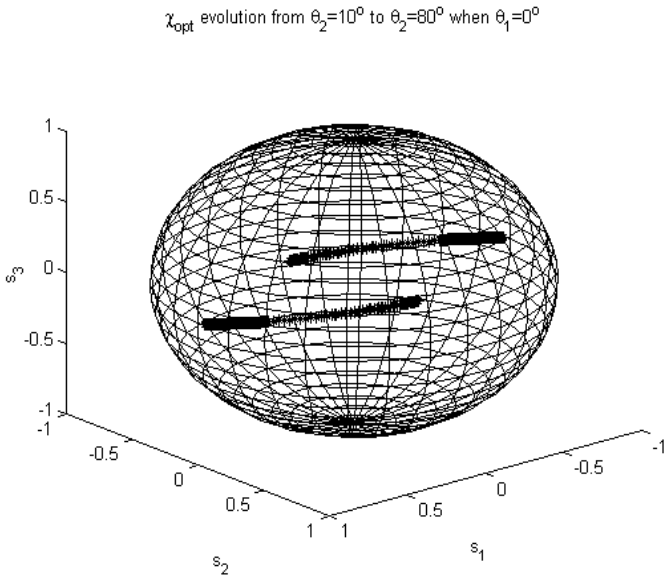

Figure 7 Optimum output state of polarization evolution with the fusion angle.

Next, θ_1 and θ_2 were rotated by 45° and the minimum σ_χ calculated. Figure 8 shows the normalized input and output pulses. As in the previous case, the narrowed output pulse carries only a small fraction of the power in the input pulse.

Finally, we simulated[14] an optical fiber made up of 500 sections of Hi-Bi fiber, each with different, uniformly distributed, values of DGD and fusion angles.

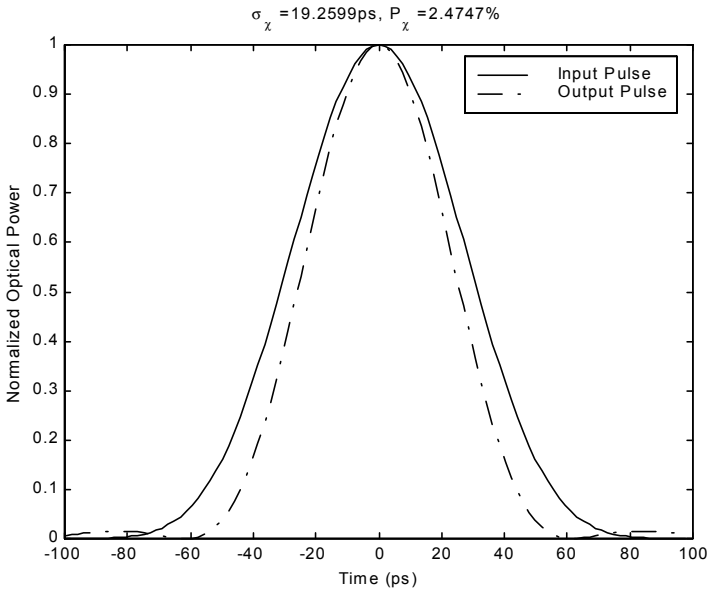

Figure 8 Input and Output pulses for the $\theta_1 = \theta_2 = 45^o$ case.

Figure 9 shows the narrowed pulse obtained for such a fiber when its mean[15] DGD equals 35 ps. In this case it was possible to obtain a sharp reduction of the pulsewidth, of 9.018 ps, at the expense of high power loss.

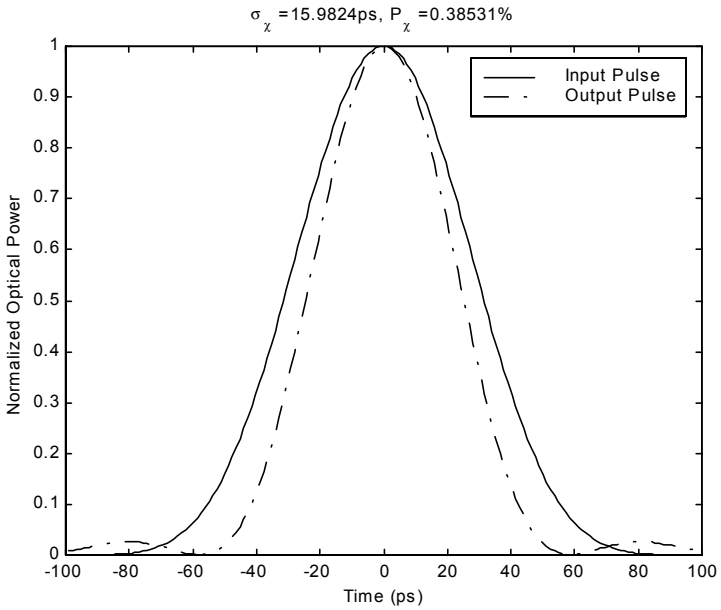

Figure 9 Pulsewidth reduction for a fiber with a mean DGD of 35 ps.

For the comparison, Figure 10 shows the input pulse, the narrowed output pulse obtained through our algorithm and the pulse that is obtained when transmitting and receiving the signal in one of the input and output PSPs[1] at the carrier frequency. The fiber simulated had a high mean DGD of 90 ps and consisted of 500 segments of Hi-Bi fiber.

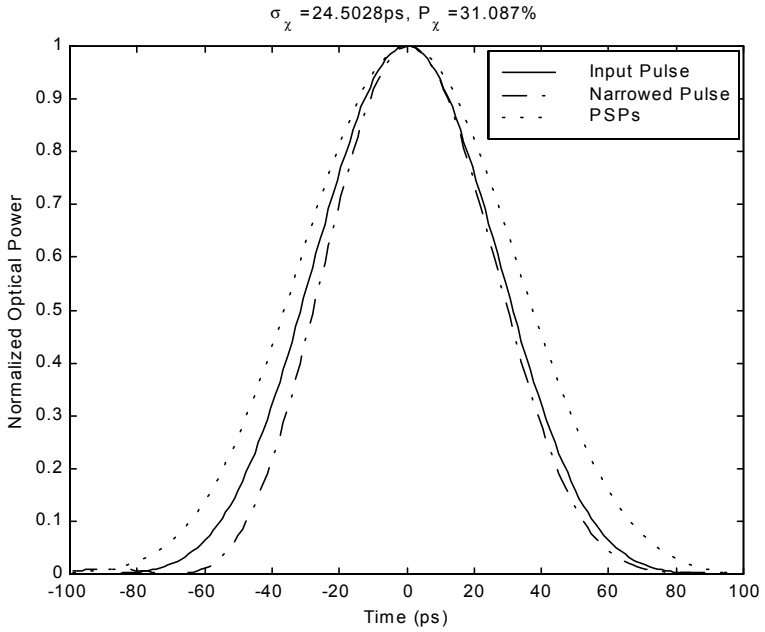

Figure 10 Input pulse, optimized output pulse and output pulse obtained by using the PSPs.

In this case the rms-pulsewidth of the signal obtained by using the PSPs was 30.377 ps, which means a pulse broadening of 5.37 ps, whilst the pulse obtained through the optimization of the launching, $\boldsymbol{\varphi}$, and reception, $\boldsymbol{\chi}$, SOP (by using our searching algorithm) did not experience any broadening, and was able to achieve a modest pulse narrowing of 0.497 ps. The power level of our narrowed pulse, 31.09%, was however significatively smaller than the power level of the broadened pulse transmitted and received on the PSPs, 90.88%.

5. SUMMARY AND CONCLUSIONS

In this paper we have presented the mathematical analysis required to minimize the rms-pulsewidth of a signal transmitted through an optical fiber with PMD by varying the input and output SOP. The analysis is quite general, is valid for any orders of PMD and does not make any assumptions about the shape of the transmitted signal. We have also described a searching algorithm capable of finding the optimum input and output SOP which minimize the rms-pulsewidth of the output signal for any given fiber. Through computer simulation we established the existence of two mutually orthogonal input and output SOP under which the rms-pulsewidth is minimized. In all our simulations the beneficial pulse narrowing effect was achieved at the expense of a sensitive reduction in the optical power of the received signal. We finally presented an example in which the use of input and output SOP different from the input and output PSPs[1] can produce a better signal at the receiving end when proper amplification is available.

6. REFERENCES

[1] C.D. Poole and R.E. Wagner, "Phenomenological approach to polarisation mode dispersion in long single mode fibers," *Electronics Letters*, Vol. 22, No. 19, pp. 1029-1030, September 11, 1986

[2] H. Sunnerud, M. Karlsson and P. Anderkson, "Analytical Theory for PMD-Compensation," *IEEE Photonics Technology Letters*, Vol. 12, No. 1, pp. 50-52, January 2000

[3] C. Francia, F. Bruyère, J. Thiéry and D. Penninckx, "Simple dynamic polarisation mode dispersion compensator," *Electronics Letters,* Vol. 35, No. 5 pp. 414-415, March 1999

[4] D. Watley, K. Farley, B. Shaw, W. Lee, G. Bordogna, A. Hadjifotiou and R. Epworth, "Compensation of polarisation-mode dispersion exceeding one bit period using single high-birefringent fiber," *Electronics Letters*, Vol. 35, No. 13,

pp. 1094-1095, June 1999

[5] T. Takahashi, T. Imai and M. Aiki, "Automatic compensation technique for timewise fluctuating polarisation mode dispersion in in-line amplifier systems," *Electronics Letters*, Vol. 30, No.4, pp. 348-349, February 1994

[6] F. Heismann, D. Fishman and D. Wilson, "Automatic compensation of first-order polarization mode dispersion in a 10 Gb/s transmission system," in *Technical Digest, European Conference on Optical Communications*, Madrid, Spain, pp. 529-530, September 1998

[7] C.D. Poole and R.C. Giles, "Polarization-dependent pulse compression and broadening due to polarization dispersion in dispersion-shifted fiber," *Optics Letters*, Vol. 13, No. 2, pp. 155-157, February 1988

[8] J. Cameron, L. Chen and X. Bao, "Anomalous pulse-width narrowing with first-order compensation of polarization mode dispersion," to appear in *Optics Letters*

[9] Z. Haas, C.D. Poole, M. Santoro and J.H. Winters, "Fiber-optic polarization dependent distortion compensation," *United States Patent*, patent number: 5,311,346 May 10, 1994

[10] M. Karlsson, "Polarization mode dispersion-induced pulse broadening in optical fibers," *Optics Letters*, Vol. 23, No. 9, pp. 688-690, May 1998

[11] W. Shieh, "Principal States of Polarization for an Optical Pulse," *IEEE Photonics Technology Letters*, Vol. 11, No. 6, pp. 677-679, June 1999

[12] L. Chen. "Minimum pulse broadening by optimizing by launch and receiver polarization in single mode fiber with polarization mode dispersion," *Internal Technical Report*, Department of Physics, The University of New Brunswick, Unpublished

[13] J. Winters, Z. Haas, M. Santoro and A. Gnauck, "Optical equalization of polarization dispersion," in *Proceedings, Multigigabit Fiber Communications, SPIE*, Vol. 1787, pp. 346-357, 1992

[14] J. Elbers, C. Glingener, M. Düser and E. Voges, "Modelling of polarisation mode dispersion in singlemode fibers," *Electronics Letters*, Vol. 33, No. 22, pp. 1894-1894, October 1997

[15] C.D. Poole and D. Favin, "Polarization-Mode Dispersion Measurements Based on Transmission Spectra Through a Polarizer," *IEEE Journal of Lightwave Technology*, Vol. 12, No. 16, pp. 917-929, June 1994

[16] J. G. Proakis, "*Digital Communications*," Third Edition, New York, NY, USA: McGraw-Hill, 1995